Available online at www.sciencedirect.com

ScienceDirect

Journal of the European Ceramic Society 27 (2007) 3697–3700

www.elsevier.com/locate/jeurceramsoc

# Fabrication and properties of textured Bi-based cobaltite thermoelectric rods by zone melting

A. Sotelo[a,*], E. Guilmeau[b], M.A. Madre[a], S. Marinel[b], J.C. Diez[a], M. Prevel[b]

[a] *Instituto de Ciencia de Materiales de Aragón (UZ-CSIC), Dpto. Ciencia y Tecnología de Materiales y Fluidos,*
*C/M$^a$ de Luna, 3, 50018 Zaragoza, Spain*
[b] *Crismat Laboratory, UMR 6508 CNRS-ENSICAEN, 6 Bd Maréchal Juin, 14050 CAEN, Cedex, Spain*

## Abstract

The performance of a thermoelectric material can be increased when the electrical conductivity is raised. This could be performed by aligning grains along a preferential direction using, for example, the laser floating zone (LFZ) method. This technique has indeed demonstrated its potentiality to increase the electrical conductivity on various ceramic materials. Moreover, with this technique, it is possible to grow samples at higher rates than with other techniques owing to the large thermal gradients developed at the melt-solid interface. The large grain sizes obtained by LFZ lead to samples with improved properties. This paper reports the synthesis of thermoelectric bars by the LFZ technique. The properties (electrical resistivity ($\rho$) and thermopower) of directionally solidified Bi-based cobaltite rods are determined and correlated with the structural features (XRD and SEM-EDX).

*Keywords:* Thermoelectric oxides; Electrical properties; Thermal conductivity

## 1. Introduction

Thermoelectric materials can be used to transform thermal to electrical energy owing to the well known Seebeck effect. This physical property allows producing electrical power from a thermal gradient between the cold and the hot side of a thermoelectric system. The performance of such materials is quantified by the figure of merit $Z$, which is defined as $S^2/\rho\kappa$, where $S$ is the Seebeck coefficient, $\rho$ the electrical resistivity, and $\kappa$ is the thermal conductivity. As all these parameters are linked and tend to vary on inverse ways, it is difficult to improve the $Z$-value. The improvement of the conversion efficiency of the thermoelectric system is then carried out by increasing the temperature difference between the hot and the cold side of the system. This is possible when the thermoelectric system can operate at high temperature for long-term use, usually under air. This application can be achieved using thermoelectric oxide ceramics, and it has been the main reason of the intense research effort put on the thermoelectric oxides. Several oxide systems have been investigated, such as $La_{1-x}Sr_xCoO_3$,[1] (Ca, Ln)$MnO_3$,[2] but the values of Z for most of these systems are smaller than for alloys and semiconductors.[3] In the case of the cobaltite phases such as $Na_xCo_2O_4$,[4] $Ca_3Co_4O_9$,[5] and $Bi_2Sr_2Co_2O_x$,[6] the situation seems to be unusual due to their large thermoelectric power. The structure of the last one is very similar to that of the Bi-family superconductors and it is well established that the LFZ technique is convenient to achieve a preferential grains orientation in these systems. It is then expected a lowering of the electrical resistivity in a view of improving their thermoelectric performances. Here is reported the processing of long textured Bi-based cobaltite bulk ceramics by the laser floating zone (LFZ) technique.[7,8] Long lengths (more than 20 cm) of textured materials have been processed. The microstructural characterization of the textured ceramics has been performed by scanning electron microscopy (SEM) equipped with EDX, and the phases were determined by powder X-ray diffraction (XRD). The thermoelectric properties were also measured and correlated with the microstructure.

## 2. Experimental

Polycrystalline ceramics with the initial composition $Bi_{1.8}Pb_{0.2}Sr_2Ca_2Co_3O_x$ were prepared by the conventional solid-state synthesis technique from commercial $Bi_2O_3$ (Panreac, 98+%), PbO (Panreac, 99+%), $SrCO_3$ (Panreac, 98+%),

---

[*] Corresponding author. Tel.: +34 976 76 2617; fax: +34 976 76 1957.
*E-mail address:* asotelo@unizar.es (A. Sotelo).

0955-2219/$ – see front matter © 2007 Elsevier Ltd. All rights reserved.
doi:10.1016/j.jeurceramsoc.2007.02.020

$CaCO_3$ (Panreac, 98.5+%) and $Co_2O_3$ (Aldrich, 98+%) powders.

These powders were weighed in the adequate proportions, mixed, milled in an agate ball mill for 30 min at 60 rpm, and calcined at 750 °C for 12 h in air to assure the carbonates decomposition. The resulting powder was subsequently carefully ground in an agate mortar, followed by a ball milling for 30 min at 60 rpm to assure good homogeneity of the mixture. The obtained product was then introduced in a furnace at 800 °C for 12 h in air, reground and ball milled to obtain a fine powder, which was isostatically pressed at 200 MPa in order to obtain green ceramic cylinders. These cylinders have been then heated at 800 °C for several hours, and quenched at room temperature in air, to improve their mechanical properties as they have to be used as feed in a LFZ device[7] equipped with a power Nd:YAG continuous laser (1.06 μm). The growth was performed downwards at a fixed growth rate of 40 mm/h and relative rotation, between feed and seed, of 18 rpm, leading to long (more than 20 cm) and textured cylindrical rods.

Powder X-ray diffraction diagrams of the final products were recorded at room temperature using a Philips diffractometer working with Cu Kα radiation. SEM images were recorded in a Philips XL 30 FEG. Electrical resistivity measurements were performed by the standard dc four-probe technique from −268.15 (5 K) to 126.85 °C (400 K) at self-field in a physical properties measurement system (PPMS) from Quantum Design. Thermopower measurements were performed with an experimental setup described elsewhere.[9]

## 3. Results and discussion

Fig. 1 shows the transversal fracture of the textured bars. It can be observed in Fig. 1a that the front growth has generated a circular arrangement of the platelets around the bar axis. This observation highlights the planar texture developed during the LFZ process, with the *c*-axis of the plate like grains aligned perpendicular to the bar axis. In Fig. 1b, a close view of the fracture shows large platelet-like grains, with dimensions exceeding 30 μm in the *ab* planes along the bar axis, and around 1 μm in the *c* direction, perpendicular to the bar axis. From the microstructural point of view, the LFZ technique demonstrated its efficiency for producing high textured bars for the first time in this type of materials.

In order to determine the phases present in the samples, powder X-ray diffraction of the final product has been recorded. In Fig. 2, it can be clearly seen that major peaks correspond to the misfit cobaltite $(Bi, Pb)_2(Sr, Ca)_2Co_{1.7}O_x$ whose general monoclinic structure is described by two sublattices with their different *b* parameters: $a = 4.90$ Å, $b_1 = 4.73$ Å, $b_2 = 2.80$ Å, $c = 14.66$ Å, $\beta = 93°49$.[10] The secondary phase $(Sr, Ca)CoO_3$ is also observed accordingly to the difference of composition between the studied precursor and the cobaltite ones. EDS analyses confirmed the presence of this secondary phase. The distribution of these secondary phases is very homogeneous in the bar, as it can be seen in Fig. 1a as dark contrast, even if the periphery exhibits a little higher concentration of these phases, due to their higher melting point.

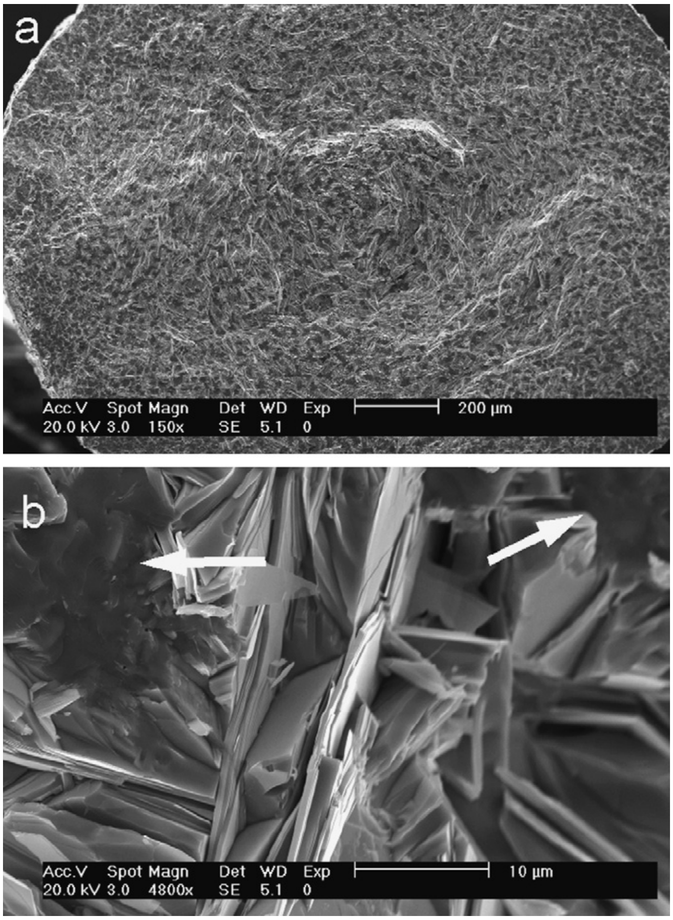

Fig. 1. SEM micrographs of transversal sections in fractured samples. (a) General view, showing the planar texture and the distribution of the secondary phases (dark contrast); (b) close view of the platelike grains. The arrows indicate the secondary phases.

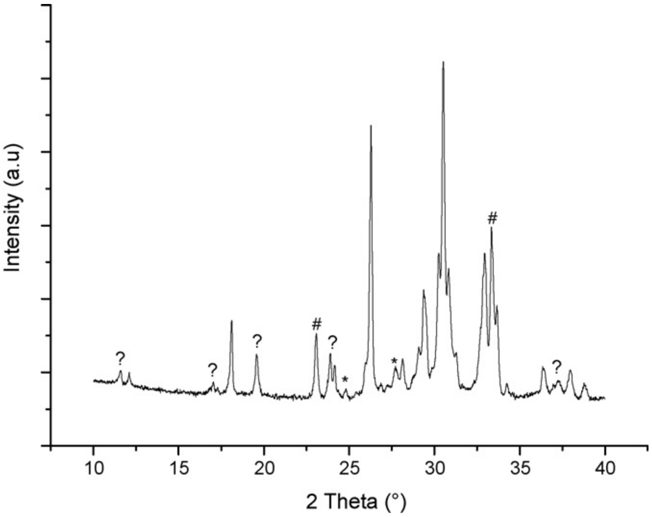

Fig. 2. Powder XRD pattern of the final textured material. Major peaks correspond to the misfit cobaltite $(Bi, Pb)_2(Sr, Ca)_2Co_{1.7}O_x$. (#) $(Sr, Ca)CoO_3$, (*) BiO, and (?) undetermined.

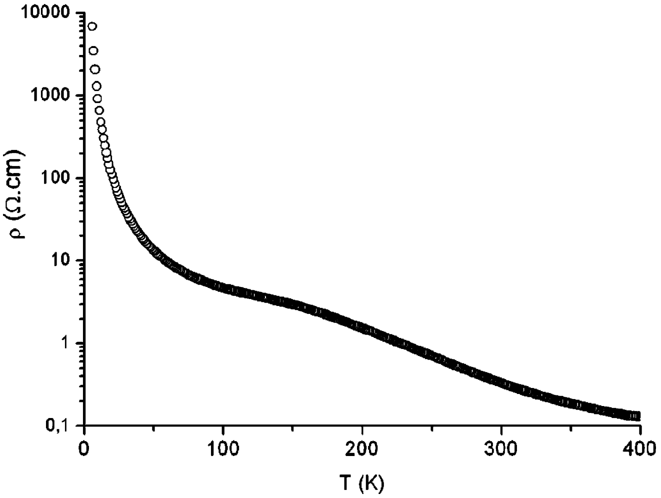

Fig. 3. Temperature dependence of the electrical resistivity, $\rho$.

The temperature ($T$) dependence of the resistivity ($\rho$) of the textured material is shown in Fig. 3. As it can be easily seen, the $\rho(T)$ curve exhibits a semiconductor behaviour from 126.85 °C (400 K) to low temperature, −268.15 °C (5 K). This falls in agreement with earlier reports[11–14] on the thermoelectric oxides. The slight increase around −73.15 °C (200 K) is certainly related to the presence of secondary phases in the material. The value at room temperature is about 80 mΩ cm, which is slightly higher than the resistivities reported in the sintered specimens.

Fig. 4 shows the variation of the thermopower with the temperature, of the as-processed BiPbSrCaCoO thin rods. It can be clearly seen that the sign of the thermopower is positive for the entire measured temperature range, which indicates a mechanism involving hole conduction.[15–19] The values of the thermopower increased from low temperature, −268.15 °C (5 K) to −73.15 °C (200 K), where a maximum of about 140 μV/K is reached. From −73.15 °C (200 K) to room temperature, a slight decrease of the thermopower is found. This effect has been associated to the presence of the secondary phases in the bulk material, as it is also discussed in the case of the resistivity measurements.

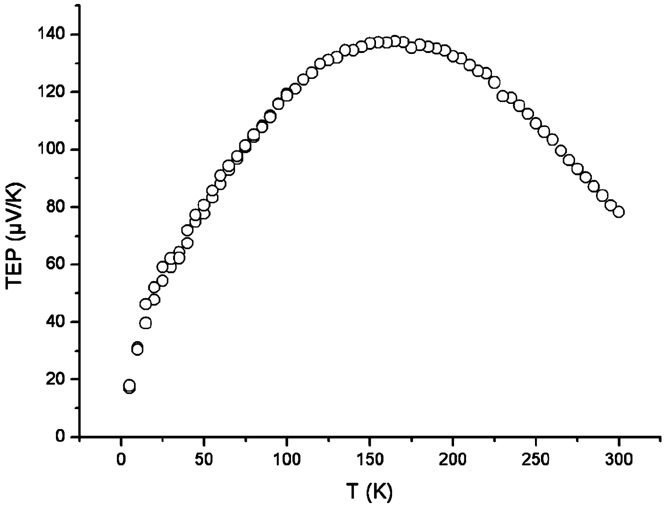

Fig. 4. Temperature dependence of the thermopower.

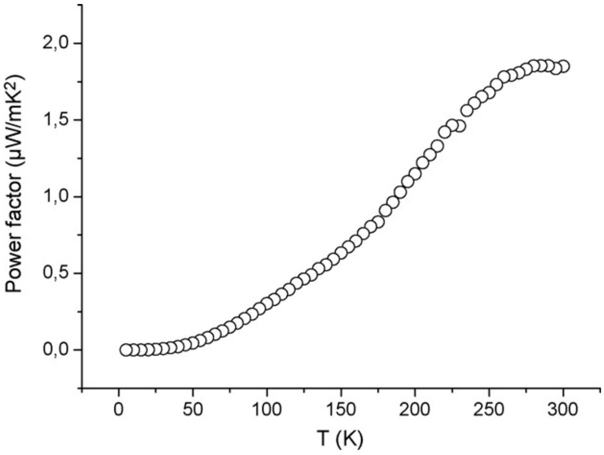

Fig. 5. Temperature dependence of the power factor, $S^2/\rho$.

In order to evaluate the thermoelectric performance of the material, the power factor $S^2/\rho$ has been calculated. The temperature dependence of the power factor estimated from the data represented in Figs. 3 and 4 is plotted in Fig. 5. The value of approximately 1.9 μW/m K$^2$ at 16.85 °C (290 K) is low compared to other reported values, due to the high value of the electrical resistivity.

## 4. Conclusions

The LFZ technique has shown to be a very useful technique for texturing thermoelectric materials for the first time, to our knowledge. The physical properties are in agreement with the literature whereas the processing has to be optimized in order to obtain a decrease of the resistivity. On the other hand, new compositions close to the cobaltite system have to be investigated with the objective of decreasing the amount of secondary phases in the bulk material.

## Acknowledgements

The authors wish to thank the Gobierno de Aragón (Consolidated Research Groups T12 and E03) for financial support. The technical contributions of C. Estepa and J.A. Gómez are also acknowledged.

## References

1. Señarís-Rodriguez, M. A. and Goodenough, J. B., Magnetic and transport properties of the system $\mathrm{La_{1-x}Sr_xCoO_{3-(}}$ ($0 < x \le 0.50$). *J. Solid State Chem.*, 1995, **116**, 224–231.
2. Ohtaki, M., Ogura, D., Eguchi, K. and Arai, H., Electrical-transport properties and high-temperature thermoelectric performance of $\mathrm{(Ca_{0.9}M_{0.1})MnO_3}$ (M = Y, La, Ce, Sm, In, Sn, Sb, Pb, Bi). *J. Solid State Chem.*, 1995, **120**, 105–111.
3. Kobayashi, T., Takizawa, H., Endo, T., Sato, T. and Shimada, M., Metal-insulator-transition and thermoelectric properties in the system $\mathrm{(R_{1-x}Ca_x)MnO_{3-(}}$ (R = Tb, Ho, Y). *J. Solid State Chem.*, 1991, **92**, 116–129.
4. Terasaki, I., Sasago, Y. and Uchinokura, S. K., Large thermoelectric power in $\mathrm{NaCo_2O_4}$ single crystals. *Phys. Rev. B*, 1997, **56**, 12685–12687.

5. Li, S. W., Funahashi, R., Matsubara, I., Ueno, K., Sodeoka, S. and Yamada, H., High temperature thermoelectric properties of oxide $Ca_9Co_{12}O_{28}$. *J. Mater. Chem.*, 1999, **9**, 1659–1660.
6. Funahashi, R., Matsubara, I. and Sodeoka, S., Thermoelectric properties of $Bi_2Sr_2Co_2O_x$ polycrystalline materials. *Appl. Phys. Lett.*, 2000, **76**, 2385–2387.
7. de la Fuente, G. F., Diez, J. C., Angurel, L. A., Peña, J. I., Sotelo, A. and Navarro, R., Wavelength dependence in laser floating-zone processing—a case study with Bi-Sr-Ca-Cu-O superconductors. *Adv. Mater.*, 1995, **7**, 853–856.
8. Huang, Y., de la Fuente, G. F., Sotelo, A., Badía, A., Lera, F., Navarro, R. *et al.*, (Bi, Pb)$_2Sr_2Ca_2Cu_3O_{10+(}$ superconductor composites—ceramics vs fibers. *Phys. C*, 1991, **185–189**, 2401–2402.
9. Hejmanek, J., Jirak, Z., Marysko, M., Martin, C., Maignan, A., Hervieu, M. *et al.*, Interplay between transport, magnetic, and ordering phenomena in $Sm_{1-x}Ca_xMnO_3$. *Phys. Rev. B*, 1999, **60**, 14057–14065.
10. Guilmeau, E., Pollet, M., Grebille, D., Hervieu, M., Muguerra, H., Cloots, R., Mikami, M. and Funahashi, R., Nano-block coupling effect in Iodine intercalated $[Bi_{0.82}CaO_2]_2[CoO_2]_{1.69}$ layered cobaltite. Inorgan. Chem. Accepted for publication.
11. Masset, A. C., Michel, C., Maignan, A., Hervieu, M., Toulemonde, O., Studer, F. *et al.*, Misfit-layered cobaltite with an anisotropic giant magnetoresistance $Ca_3Co_4O_9$. *Phys. Rev B*, 2000, **62**, 166–175.
12. Yamamoto, T., Tsukada, I., Uchinokura, K., Takagi, M., Tsubone, T., Ichihara, M. *et al.*, Structural phase transition and metallic behaviour in misfit layered (Bi, Pb)-Sr-Co-O system. *Jpn. J. Appl. Phys.*, 2000, **39**, L747–L750.
13. Funahashi, R., Urata, S., Sano, T. and Kitawaki, M., Enhancement of thermoelectric figure of merit by incorporation of large single crystals in $Ca_3Co_4O_9$ bulk materials. *J. Mater. Res.*, 2003, **18**, 1646–1651.
14. Fujii, T., Terasaki, I., Watanabe, T. and Matsuda, A., Large in-plane anisotropy on resistivity and thermopower in the misfit layered oxide $Bi_{2-x}Pb_xSr_2Co_2O_y$. *Jpn. J. Appl. Phys.*, 2002, **41**, L783–L786.
15. Terasaki, I., Sasago, Y. and Uchinokura, K., Large thermoelectric power in $NaCo_2O_4$ single crystals. *Phys. Rev. B*, 1997, **56**, 12685–12687.
16. Funahashi, R. and Matsubara, I., Thermoelectric properties of Pb- and Ca-doped $(Bi_2Sr_2O_4)_xCoO_2$ whiskers. *Appl. Phys. Lett.*, 2001, **79**, 362.
17. Masuda, Y., Nagahama, D., Itahara, H., Tani, T., Seo, W. S. and Koumoto, K., Thermoelectric performance of Bi- and Na-substituted $Ca_3Co_4O_9$ improved through ceramic texturing. *J. Mater. Chem.*, 2003, **13**, 1094–1099.
18. Itoh, T. and Terasaki, I., Thermoelectric properties of $Bi_{2.3-x}Pb_xSr_{2.6}Co_2O_y$ single crystals. *Jpn. J. Appl. Phys.*, 2000, **39**, 6658–6660.
19. Funahashi, R., Matsubara, I., Ikuda, H. and Takeuchi, T., An oxide single crystal with high thermoelectric performance in air. *Jpn. J. Appl. Phys.*, 2000, **39**, L1127–L1129.